NUMERICAL INVESTIGATION OF PRODUCTION-RELATED CHARACTERISTICS REGARDING THEIR INFLUENCE ON THE FATIGUE STRENGTH OF ADDITIVELY MANUFACTURED COMPONENTS

Michaela ZEIßIG* , **Frank JABLONSKI****

*Faculty of Production Engineering, Bremen Institute for Mechanical Engineering (bime), University of Bremen,
Am Biologischen Garten 2, 28359 Bremen, Germany
**Faculty 5, City University of Applied Sciences Bremen, Neustadtswall 30, 28199 Bremen, Germany

mzeissig@uni-bremen.de, Frank.Jablonski@hs-bremen.de

Abstract: In order to further enhance the application of additive manufacturing (AM) processes, such as the laser powder bed fusion (L-PBF) process, reliable material data are required. However, the resulting specimen properties are significantly influenced by the process parameters and may also vary depending on the material used. Therefore, the prediction of the final properties is difficult. In the following, the effect of residual stresses on the fatigue strength of 316L steel, a commonly used steel in AM, is investigated using a Weibull distribution. The underlying residual stress distributions as a result of the building process are approximated for two building directions using finite element (FE) models. These imply significantly different distributions of tensile and compressive residual stresses within the component. Apart from the residual stresses, the impact of the mean stress sensitivity is discussed as this also influences the predicted fatigue strength values.

Key words: additive manufacturing, fatigue strength, Weibull distribution, FEM

1. INTRODUCTION

Additive manufacturing (AM) shows great potential across various industries ranging from aerospace to medical applications. Some of its main advantages are moldless manufacturing, production of near net-shape geometries and great geometrical freedom. There are different processes which belong to the group of AM techniques. One of them is the widespread laser powder bed fusion (L-PBF) process. The component is built using repetitive cycles of powder layer distribution and selective laser melting of the powder. This happens according to a previously defined and virtually sliced geometry [1]. The process itself has numerous configurable process parameters. Among them are the building direction of the component relative to the building platform, the laser parameters like speed, power and scanning path and powder-related parameters such as the particle size, temperature and the powder layer height [1]. This multitude of parameters makes predictions of the final properties of the component difficult, especially as general assumptions for different AM materials are not possible. This means that each material needs to be investigated separately considering the process and material-related characteristics. In the following, the focus is on the fatigue strength of the austenitic steel 316L (1.4404).

2. CHARACTERISTICS OF ADDITIVELY MANUFACTURED COMPONENTS WITH RESPECT TO FATIGUE STRENGTH

Due to the manufacturing process, L-PBF components show some characteristics which are in line with the known influencing parameters on the fatigue strength. These include tensile residual stresses, high surface roughness, a specific grain structure and stress raisers such as pores and other defects [2]. These in combination with external parameters such as the loading direction and potential mean stress determine the fatigue life of a specific component [3]. Each of the characteristics has an effect on the fatigue strength; however, their influences may not be easily assessed independently because of their simultaneous occurrence in the components. In the following, the AM characteristics and their general effects on the fatigue strength will be briefly described.

2.1 Residual stresses

The repetitive process of melting and solidification in line with heating and cooling of the component leads to the development of significant tensile residual stresses, at least in the outer region of as-built components [4,5]. These have a negative impact on the fatigue strength. Postprocessing, e.g., in terms of heat treatments or hot isostatic pressing may reduce these residual stresses (for some materials) as reported in the study by Leuders et al. [6]. Knowledge about the residual stress distribution within components is required to decide whether these postprocessing procedures are necessary to achieve the required properties. Knowledge is also required if these treatments shall be avoided by minimisation of residual stresses and distortion via optimised building parameters (e.g. [7]).

2.2 Pores and other defects

The porosity of L-PBF components is usually very low. In Zhang et al. [8], the density of such components is given as around

95%, while in the study by Hatami et al. [5], the porosity determined via image analysis was even well below 0.5%. However, there are still some pores and other defects present in the component. These result from the manufacturing process and may be divided by their origin, which in turn is related to their morphologies. In the study by Zhang et al. [9], three different defect types are distinguished: pores, lack-of-fusion (LOF) defects and cracks. While pores are usually small (up to about 100 μm) and rather spherically shaped, LOF defects are rather irregularly shaped [10,11]. The pores are attributed to gas bubbles while the LOF defects are attributed to insufficient melting of the particles [11]. The defects correspond to stress concentrations and, therefore, may be potential crack initiation sites.

2.3 Surface state

Unprocessed, so-called as-built surfaces show high surface roughness. For 316L, surface roughness values are given in the study by Wang et al. [12] for Ra as between 5 and 25 μm, while the value depends on the manufacturing parameters. Furthermore, the surface roughness varies with the orientation of the surface relative to the building direction. In addition to the mere surface roughness, near-surface porosity, meaning small pores in a zone below the surface as reported in the study by Hatami et al. [5], may need to be included in the assessment of the surface state. In general, high surface roughness has a detrimental effect on the fatigue strength as it may, e.g., induce stress peaks.

2.4 Microstructure

Depending on the building parameters and the material, different types of microstructures may be found in the final component. For 316L, a cellular microstructure is typical while for other materials like Ti-6-Al-4V elongated, columnar grains are reported [13].

3. FATIGUE STRENGTH EVALUATION OF L-PBF COMPONENTS

As stated above, various factors influence the fatigue strength of a component built via the L-PBF process. In the following, a Weibull distribution [14,15] which is often applied for fatigue assessment will be used. Here, it is applied in such a way that it explicitly incorporates the effect of residual stresses and inherently the effect of defects present in the component.

3.1 Weibull distribution

The Weibull distribution is a probability density function based on the assumption that every component initially includes randomly distributed defects. Furthermore, fatigue failure is defined as crack initiation. This in turn is supposed to take place if the local stress exceeds the local material endurance.

For an individual volume element ΔV of a component with the total volume V_0, the survival probability is calculated according to the following equation:

$$P_{\text{survival},\Delta V} = 2^{-(\Delta V/V_0)(\sigma_{\text{Mises}}/\sigma_{\text{WV}})^{m_V}} \tag{1}$$

with σ_{Mises} being the equivalent stress amplitude and σ_{WV} representing the local fatigue limit. The Weibull exponent m_V is used to fit the effect of size and scattering of the defects present in the component [16].

The residual stresses σ_i^{RS} are accounted for as part of the material resistance [17,18], not as part of the material loading. Consequently, part of the exponent of Eq. (1) can be rewritten as follows:

$$\frac{\sigma_{\text{Mises}}}{\sigma_{\text{WV}}} = \frac{\sigma_{\text{Mises}}}{\sigma_{\text{WV}} - M \cdot (\sigma_1^{\text{RS}} + \sigma_2^{\text{RS}} + \sigma_3^{\text{RS}})} \tag{2}$$

The impact of the residual stresses is influenced by the residual stress sensitivity M. According to [3], it may be assumed equal to the mean stress sensitivity following the assumption that the impact of residual stresses is comparable to that of mean stresses. For non-welded components, M can be determined based on the ultimate tensile strength R_m as follows:

$$M = a_M \cdot 10^{-3} \cdot \frac{R_m}{\text{MPa}} + b_M \tag{3}$$

with a_M and b_M being material constants. For steel, the constants take on the values 0.35 and −0.1, respectively [19]. Using the values from Tab. 1, M is calculated to be about 0.14 for the horizontal and 0.11 for the vertical building direction. In addition, a common value used for M is 0.3. It corresponds to the value given in the FKM guideline [19] for the state of low residual stresses within a welded component. However, as the values measured in the study by Hatami et al. [5] and the values obtained via the approximations using finite element (FE) models below both suggest residual stresses above the threshold of $0.2 \cdot R_p$ (see Tab. 1), the assumption of low residual stresses seems not to be valid. However, in order to assess the impact of the residual stress sensitivity on the fatigue predictions using Weibull distributions, it will be included in the calculations below.

Moreover, the application of Eq. (2) requires the local fatigue limit σ_{WV}. This value refers to the fatigue limit without influencing factors such as residual stresses. Therefore, the value is approximated using the relation between the ultimate tensile strength and the fatigue strength. A factor of 0.4 is assumed [19]. Furthermore, the Weibull exponent m_V is set to 20. The required input data regarding the residual stress distribution is obtained via FE calculations as described in the following.

3.2 Approximation of residual stress distribution

The unnotched fatigue specimen used has a length of about 50 mm and a smallest diameter of 4 mm. The material used is 316L steel, an austenitic steel commonly used in AM due to its wide applicability and its comparably easy handling. The main material parameters used for the Weibull approach are given in Tab. 1. As one can see, the material data have a dependency from the building direction of the component. This applies to the static values and may also be valid for the fatigue strength.

The residual stress data were obtained via a rough approximation using the Abaqus Welding Interface (AWI) [21], an extension to Abaqus [22]. For the calculations, Poisson's ratio was assumed as 0.3, and material data implemented in the AWI [21], similar to that of 316L steel, were supplemented. Sequentially coupled calculations have been carried out, neglecting the scanning strategy, combining several component layers of typical height around 50 μm [5] and adding them as a whole. The thermal history

sciendo

Michaela Zeißig, Frank Jablonski

Numerical Investigation of Production-Related Characteristics Regarding their Influence on the Fatigue Strength of Additively Manufactured Components

DOI 10.2478/ama-2023-0033

is obtained via the first calculation and subsequently used as input for the second calculation in order to obtain the stress distribution. Afterwards, the component is removed from the building platform, and the axial stress distributions along a path through the middle of the specimen as shown in Fig. 1 are obtained.

Tab. 1. Material data for 316L steel with respect to building direction taken, adapted from Gläßner et al. [20].

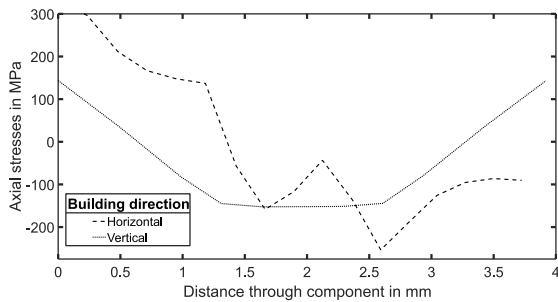| Characteristics	Horizontal manufac-turing direction	Vertical manufac-turing direction
Young's modulus	167 GPa	152 GPa
R_m	681 MPa	612 MPa
$R_{p0.2}$	609 MPa	490 MPa

Fig. 1. Axial residual stress approximation along a path through the smallest cross section of the fatigue specimen for the vertical and horizontal building directions.

Although the FE calculations using the AWI [21] are only a rough approximation and are also related to the specimen geometry and the process parameters, which are mostly not included in the approximations, the values are in general agreement with those reported for the near surface area of a fatigue specimen made of 316L steel in the study by Hatami et al. [5]. The stresses in longitudinal direction reported in the study by Hatami et al. [5] for an as-built specimen are given as about 300 MPa and 600 MPa, depending on the process parameters. They were measured up to a depth of around 100 μm. Due to the mesh size, data in comparable steps are not available; however, the general size seems to agree. For the vertically built specimen, the axial stresses seem to be quite symmetric with respect to the longitudinal axis, while the stresses in the horizontally built specimen change from tensile to compressive from the top to the bottom (orientation during the building process). Comparing both curves, the stresses within the horizontally built component are predicted higher, both tensile and compressive, and the component also shows larger areas of compressive stresses than the vertically built specimen. Reasons for the change of direction of the horizontal curve around 2.5 mm and its stepwise shape might be the removal from the platform, the chosen layer height and mesh size, although a more symmetrical shape would be expected. Again, the overall FE results seem to be in general agreement regarding the tensile amount near the surface; however, experimental validation is required.

3.3 Results and discussion

According to Eq. (1), the fatigue limit for a 50% survival probability of the whole component will be determined. Although the

absolute values of residual stresses and calculated fatigue strength may not be used for direct comparison and prediction, the influence of the residual stress sensitivity can be evaluated. Fig. 2a shows the survival probability distribution of the vertically built specimen under consideration of the approximated residual stress distribution. Furthermore, different stress sensitivity values are evaluated. In Fig. 2b, the results for the horizontally built specimen are shown. The predicted fatigue limits for the vertically built specimens are lower than those for their horizontally built counterparts. This is based on the lower material properties as given in Tab. 1 and the different residual stress distribution.
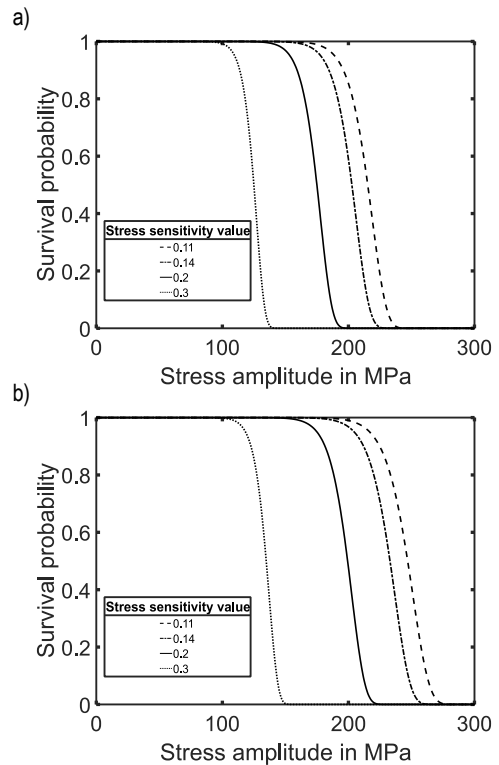

Fig. 2. Effect of different residual stress sensitivity values on the predicted fatigue survival probabilities: (a) vertically built; (b) horizontally built.

As expected, the curves are aligned according to the underlying residual stress sensitivity value from left to right starting with the highest value of 0.3. Furthermore, the curves are parallelly shifted while the shape is not affected by the stress sensitivity. The shape of the curves is determined via the Weibull exponent as shown, e.g., in the study by Zeißig and Jablonski [23]. According to Fig. 2, choosing a value of 0.3, in the absence of experimental data for this parameter, might be a very conservative approach and might unnecessarily restrict the application of components. The differences between the predicted endurable load stresses for a survival probability of 50% for the two curves on the left, with stress sensitivity values of 0.3 and 0.2, are 65 MPa and 50 MPa, respectively. Further investigations regarding the residual stress sensitivity of L-PBF components, therefore, seem to be advisable.

Fig. 3 shows the calculated fatigue stress amplitude values given in Fig. 2 in relation to the underlying fatigue strength which is taken as residual stress-free. It should be noted that according to Tab. 1, these values are different for the two manufacturing directions. Overall, the predicted reduction of the fatigue limit in terms of the base values is in the same order for both directions. However,

the difference in the calculated fatigue limit for the lowest and highest chosen residual stress sensitivity value is significant and ranges between about 50% and about 90% of the base value. Comparing this to the results stated in the study by Leuders et al. [6] where the effect of different heat treatments on the fatigue limit of 316L was investigated, the impact on the fatigue limit seems to be overestimated in the calculations.
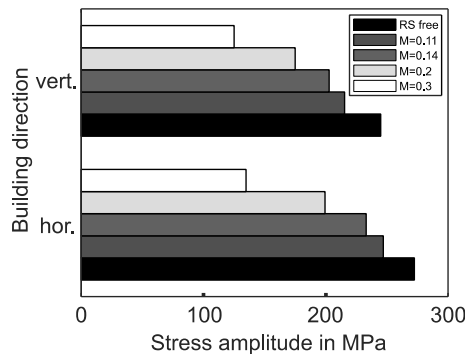

Fig. 3. Effect of different residual stress sensitivity values on the predicted fatigue stress amplitudes for vertical and horizontal building direction and considering residual stress-free state. (Survival probability of 50%).

4. SUMMARY AND OUTLOOK

As has been shown, in fatigue calculations, the effect of the residual stress sensitivity on the results should not be neglected. Experimental validation in terms of this parameter as well as for residual stress distributions of entire components seems to be necessary.

Predictions of the fatigue strength of components manufactured via L-PBF are difficult as there are numerous influencing parameters due to the building process, and their variations have an impact on the final results. Furthermore, results have no general validity for all materials as the material characteristic governing the fatigue limit may not be the same for every material; hence, individual investigations regarding each material seem to be necessary. Therefore, with respect to the shown approach, in the future, the microstructure and local deviations of the material properties should also be included in order to make it more versatile and enhance its applicability.

REFERENCES

1. Pelleg J. Additive and Traditionally Manufactured Components: A Comparative Analysis of Mechanical Properties. Amsterdam (NL): Elsevier; 2020.
2. Kruth J-P, Badrossamay M, Yasa E, Deckers J, Thijs L, Van Humbeeck J, Zhao W. Part and material properties in selective laser melting of metals. Proceedings of the 16th International Symposium on Electromachining (ISEM XVI), 2010, 3-14.
3. Radaj D, Vormwald M. Ermüdungsfestigkeit. 3rd ed. Berlin (DE): Springer-Verlag, 2007.
4. Mercelis P, Kruth J-P. Residual stresses in selective laser sintering and selective laser melting. Rapid Prototyp. J. 2006; 12(5): 254-265.
5. Hatami S, Ma T, Vuoristo T, Bertilsson J, Lyckfeldt O. Fatigue Strength of 316 L Stainless Steel Manufactured by Selective Laser Melting. J. of Materi Eng and Perform 2020; 29(5): 3183-3194.
6. Leuders S, Lieneke T, Lammers S, Tröster T, Niendorf T. On the fatigue properties of metals manufactured by selective laser melting – The role of ductility. J. Mater. Res. 2014; 29(17): 1911-1919.
7. Keller N. Verzugsminimierung bei selektiven Laserschmelzverfahren durch Multi-Skalen-Simulation [dissertation]. Bremen: University of Bremen, 2017 [cited 6 July 2017]. Available from: http://nbn-resolving.de/urn:nbn:de:gbv:46-00105808-15
8. Zhang Y, Jung Y-G, Zhang J. Multiscale Modeling of Additively Manufactured Metals: Application to Laser Powder Bed Fusion Process. Amsterdam (NL): Elsevier; 2020.
9. Zhang B, Li Y, Bai Q. Defect Formation Mechanisms in Selective Laser Melting. Chin. J. Mech. Eng. 2017; 30(3): 515-527.
10. Nadot Y, Nadot-Martin C, Kan WH, Boufadene S, Foley M, Cairney J, Proust G, Ridosz L. Predicting the fatigue life of an AlSi10Mg alloy manufactured via laser powder bed fusion by using data from computed tomography. Addit. Manuf. 2020; 32(3): 100899.
11. Mertens A, Reginster S, Paydas H, Contrepois Q, Dormal T, Lemaire O, Lecomte-Beckers J. Mechanical properties of alloy Ti–6Al–4V and of stainless steel 316L processed by selective laser melting: Influence of out-of-equilibrium microstructures. Powder Metall. 2014; 57(3): 184-189.
12. Wang D, Liu Y, Yang Y, Xiao D. Theoretical and experimental study on surface roughness of 316L stainless steel metal parts obtained through selective laser melting. Rapid Prototyp. J. 2016; 22(4): 706-716.
13. Vrancken B. Study of Residual Stresses in Selective Laser Melting [dissertation]. Leuven (BE): KU Leuven, 2016 [cited 10 May 2017]. Available from: https://lirias.kuleuven.be/1942277
14. Weibull W. A statistical theory of the strength of materials. Ingeniörsvetenskapsakademiens handlingar 151. Stockholm (SE): Generalstabens Litografiska Anstalts Förlag, 1939.
15. Weibull W. A Statistical Distribution Function of Wide Applicability. J. Appl. Mech. 1951; 18(3): 293-297.
16. Bomas H, Mayr P, Schleicher M. Calculation method for the fatigue limit of parts of case hardened steels. Materials Science and Engineering: A 1997; 234: 393-396.
17. Macherauch E, Kloos K-H. Bewertung von Eigenspannungen. Härterei-Technische Mitteilungen, Beiheft Eigenspannungen und Lastspannungen, Moderne Ermittlung – Ergebnisse – Bewertung 1982; 175-194.
18. Jablonski F. Rechnerische Ermittlung von Dauerfestigkeitskennwerten an einsatzgehärteten Proben aus 16 MnCrS 5 unter Berücksichtigung von Mittel- und Eigenspannungen [dissertation]. University of Bremen. Aachen (DE): Shaker Verlag, 2001.
19. FKM Forschungskuratorium Maschinenbau e.V. FKM-Richtlinie; Rechnerischer Festigkeitsnachweis für Maschinenbauteile. 6th ed. Frankfurt am Main (DE): VDMA-Verlag, 2012.
20. Gläßner C, Blinn B, Burkhart M, Klein M, Beck T, Aurich JC. Comparison of 316L test specimens manufactured by Selective Laser Melting, Laser Deposition Welding and Continuous Casting. In: Schmitt RH, Schuh G, editors. 7. WGP-Jahreskongress. 2017 5-6 Oct; Aachen, Germany. Aachen (DE): Apprimus Verlag, 2017; 45-52.
21. Abaqus Welding Interface 2017, User Manual, AWI Version AWI_2017-5. Dassault Systems Simulia Corp., 2018.
22. Abaqus/CAE 2017. Dassault Systemes Simulia Corp., 2016.
23. Zeißig M, Jablonski F. Comparison of different approaches to model fatigue for additively manufactured specimens considering production related characteristics. Procedia Struct. Integr. 2022; 38(5): 60-69.

Michaela Zeißig: https://orcid.org/0009-0001-8249-9495

Frank Jablonski: https://orcid.org/0000-0002-9670-0540